論文 한국공작기계학회지 제9권 제5호 2000.10.
Journal of the Korean Society of Machine Tool Engineers

턴널전류 효과를 이용한 미소가속도계의 마이크로머시닝 공정에서 온도분포 해석

김 옥 삼*

Analyses of the Temperature Distribution at Micromachining Processes for Microaccelerometer Based on Tunneling Current Effect

O. S. Kim*

Abstract

Micronization of sensor is a trend of the silicon sensor development with regard to a piezoresistive silicon pressure sensor, the size of the pressure sensor diaphragm have become smaller year by year, and a microaccelerometer with a size less than 200~300㎛ has been realized. Over the past four or five years, numerical modeling of microsensors and microstructures has gradually been developed as a field of microelectromechanical system(MEMS) design process. In this paper, we study some of the micromachining processes of single crystal silicon(SCS) for the microaccelerometer, and their subsequent processes which might affect thermal and mechanical loads. The finite element method (FEM) has been a standard numerical modeling technique extensively utilized in structural engineering discipline for component design of microaccelerometer. Temperature rise sufficiently low at the suspended beams. Instead, larger temperature gradient can be seen at the bottom of paddle part. The center of paddle part becomes about 5~20℃ higher than the corner of paddle and suspended beam edges.

Key Words : Finite element analyses, Temperature distribution, Micromachining processes, Microaccelerometer, Tunnel current effect

1. INTRODUCTION

In the past decade, much attention focused on SCS micromechanical structures, The potential for merging these structures with integrated circuits to create MEMS has been a major driving force behind the researchs.[1] Recently, there has been growing interest in micromachined silicon accelerometers for applications to automotive equipment systems such as airbag, anti-lock braking system(ABS), active suspension and navigation instrumentation.[2] Among them, airbag accelerometers open the most immediate and the largest market, whose demand for high

* Dept of Mechanical Engineering. Yosu National University.

reliability, mass production and high sensitivity to both velocity change and vibration cannot be met easily by conventional electromechanical sensor technology for airbag applications, SCS accelerometers show a strong potential due to simple detection circuit and moderate performance characteristics.

Over the past four or five years, numerical modeling of microsensors and microstructures has gradually been developed as a field of MEMS design process. The advantage of numerical analyses for prediction of device performance as well as device limitations has been verified in many problems.[3] In the design of microsensors and microstructures, a multitude of layers such as thermal oxide and coating are grown and deposited at different processes to achieve certain mechanical and/or electrical geomertris and functions. Due to different mechanical and physical properties of these layers, the device usually experiences various thermal and mechanical loading resulting in displacements and residual stresses which are often not easy to predict by experimental approaches.

Successful analysis and design of the microaccelerometer based on the tunneling current concept using silicon on insulator(SOI) wafer depend on the knowledge about normal mechanical properties of the SCS layer such as yield stress, Young's modulus and Poisson's ratio, and their control through manufacturing process.[4] However, these computer simulations seem essential for microaccelerometer analysis and design, since it is often very difficult to precisely measure physical /mechanical properties in a micro and nanoscopic world.[5]

In this paper, we study some of the micromachining processes of SCS for the microaccelerometer, and their subsequent processes which might affect thermal and mechanical loads. The FEM has been a standard numerical modeling technique extensively utilized in structural engineering discipline for component design of microaccelerometer. The FEM is becoming a standard design tool in microsensor industry.[6-7]

2. MICROACCELEROMETER BASED ON TUNNELING CURRENT CONCEPT

2.1 Microaccelerometer of Tunneling current effect

Silicon microfabricated accelerometers are being intensively developed because of the possibility of low cost batch fabrication. Fig. 1 shows a perspective of the microaccelerometer based on the tunneling current concept, where a simple suspend beam, paddle and supporting rims are micromachined from a SOI wafer {100} face. Microaccelerometer based on tunneling current concept have also been proposed, in which the sense signal is derived from a tunneling current between a sensing tip and a counter electrode. Such accelerometers have a

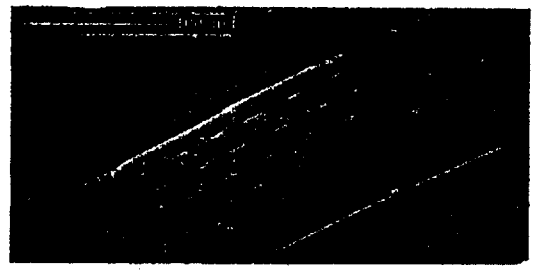

(a) SEM image for vibrating trial product of microaccelerometer

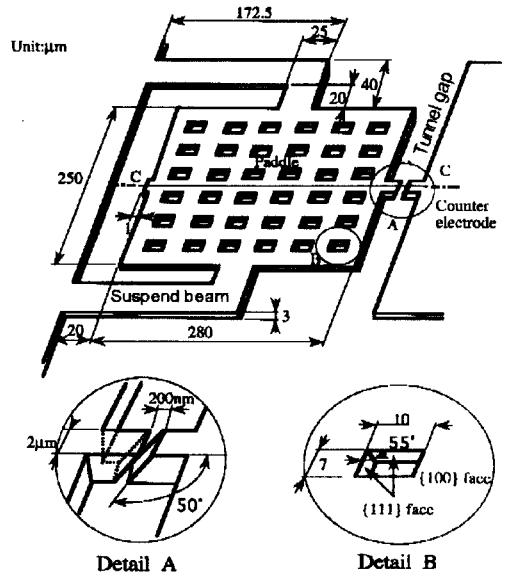

(b) Rough configuration

Fig. 1 Schematic view of microaccelerometer based on tunneling current concept

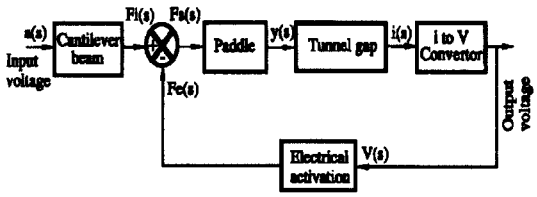

Fig. 2 Block diagram of microaccelerometer

greater sensitivity than conventional capacitive accelerometers.

The paddle of microaccelerometer having a lot of holes due to etching has the following two roles, i. e. (1) carrying an extra proof mass to enhance inertia force, and (2) producing electrostatic force as a part of condenser to control position as shown Fig. 1 (b).

Fig. 2 shows the chosen system concept for the accelerometer that uses the principle of the tunneling current to detect the acceleration a paddle. A feedback servo loop with electrical activation of the paddle is used to keep the tunnel gap constant. Acceleration $a(s)$ is initially converted into an inertial force $Fi(s)$, via paddle. This force causes a deflection in the spring $y(s)$, but this is detected by the tunneling current when the deflection exceeds a certain threshold level at sensing tip and counter electrode. The change in tunnel current, $i(s)$ converted into a feedback voltage $V(s)$, which causes an activation force $Fe(s)$, which counters the inertial force. The applied voltage must be less than 15 V, considering its supply resource. The change of applied acceleration is converted from the comp-ensation voltage. Compensation voltage for the acceleration change should be about 0.3 V. The method of electrical activation, for maintaining a constant tunnel gap, consists of electrostatic pulling between the paddle and the silicon substrate.

2.2 Micromachining processes

In the fabrication of the microaccelerometer, SOI wafer is used as a starting material. SOI wafer is promising since the top layer silicon is SCS and no assembly after the processing is necessary. Only one lithographic step and simple wet etching are required to create microstructure[8]

2.2.1 SOI wafer production

The manufacturing processes of SOI wafer which are shown Fig. 3 consists of (1) growing a thermal oxide SiO_2 layer(2㎛) on a main substrate(500㎛) and a SiO_2 layer(2㎛) on a handle substrate(SCS) of paddle, (2) bonding a haddle substrate to a main substrate during 2hr.[9] The bonding is achieved by attaching the oxidized surfaces of the two substrates eachother with pressure, and by inserting them into an oxidizing atmosphere at about 1000~1100 ℃. Typically, the substrates are pressed together to expel most of air, bubble and void in between the bonded surfaces. The handle substrate is then thinned to some extent using micro grinding and chemical micro polishing(CMP) at room temperature. SOI wafer is promising since the top layer (thickness 3㎛) silicon is single crystalline and no assembly after the processing is necessary.

2.2.2 Micromachining steps

The fabrication steps for the microaccelerometer which are shown Fig. 4 can be summarized as follows : (1) oxida-

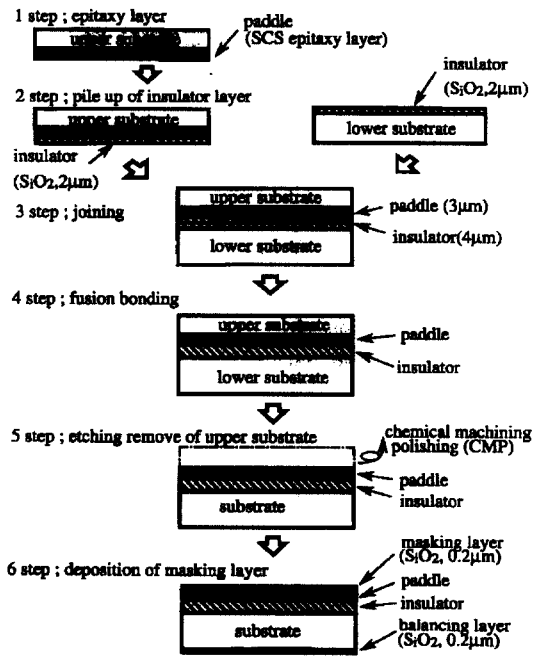

Fig. 3 Schematic of SOI wafer producing processes

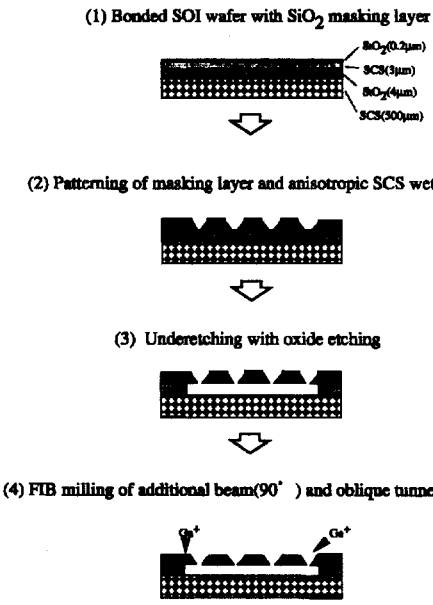

Fig. 4 Micromachining steps for the microaccelerometer based on tunneling current concept

tion of the SOI wafer to create a masking layer (0.2㎛), (2) anisotropic wet etching of the top Si layer of 3㎛ thickness with KOH, (3) wet etching in HF(conc.) to undercut the paddle(4㎛) with silicon oxide (SiO_2) layer, and (4) FIB(focused ion beam) cut to mill the tunnel gap and to fully release the paddle. The tunnel gap is machined to have a gap width of 200㎚ by the FIB technology. The deposition of an appropriate metal layer(Pt) will be necessary as a final step to assure good contact surface in the tunnel gap.[10]

3. COMPUTATIONAL MODELING

Algorithms of computational procedures for temperature distributions occurred in SOI wafer and microaccelerometer manufacturing process are unconditionally stable and accurate for moderate strain increments. We seek for the general structure of the governing equation. Stress calculations also assume that the vertical temperature gradient in the microaccelerometer can be ignored. The thermal stress is caused due to the temperature gradient of SCS, SiO_2 and substrate with different thermal expansion coefficients. This is not discussed in this paper. We consider the thermally epitaxial grown layer of oxide, the underetching of SiO_2 and the FIB milling of additional beam(90°) and oblique tunnel gap (50°), referring to Table 1.

Table 1 Cyclic thermal loadings during micromachining processes

Process	Temp. (℃)	Duration (sec)	Appliance	Working area
FIB cutting	100	54	FIB	Tunnel gap
FIB cutting	80	20	FIB	Additional beam
Pt deposition	400	120	CVD*	Tunnel gap

*** Chemical Vapor Deposition**

The analytical approach to microsensors is only possible for simple structures. More complex shapes involing beams or multiple layer elements are best handled by finite element techniques. The paddle part is 280㎛ along, 250㎛ wide and 3㎛ thick. In the analysis the microaccelerometer volume is divided into 143 rectangular(8-node) elements. Analysis of this microaccelerometer using MARC K6.1 code, generates heat transfers and thermal stresses in a transient state.

4. RESULTS AND DISCUSSIONS

Fig. 5 show the calculated temperature profiles of microaccelerometer at the tunnel gap at heating by FIB after 2.2×10^{-6}sec. The distributions illustrate the contours concentration of temperature near the corner of paddle according to heat source about 100℃.

Fig. 6 shows the temperature distribution of a heating process in additional beam for FIB cutting(90°) at approximately heating after 4.8×10^{-9}sec. Temperature rise sufficiently low at the suspended beams. Instead, larger temperature gradient can be seen at the bottom of paddle part.

The temperature contours of Pt deposition heating process for the tunnel gap are depicted in Fig. 7 after 1.3×10^{-6}sec. The typical heating behavior curves are shown in this figure.

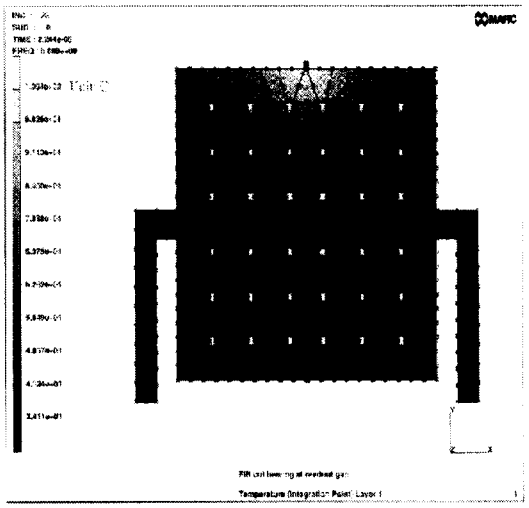

Fig. 5 Temperature distribution after 2.2×10^{-4} sec of heating process for tunnel gap by FIB cutting (50°)

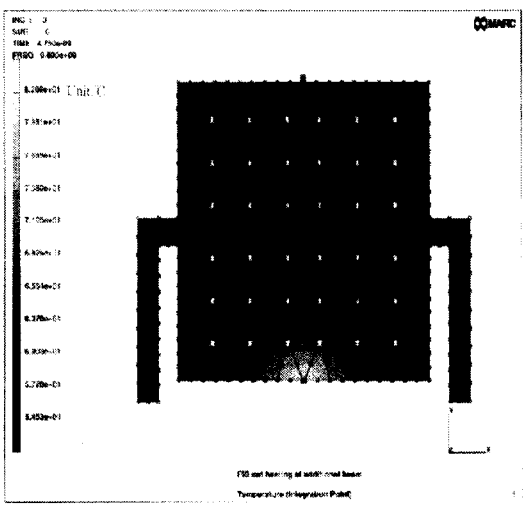

Fig. 6 Temperature distribution after 4.8×10^{-5}sec of heating process for additional beam by FIB cutting (90°)

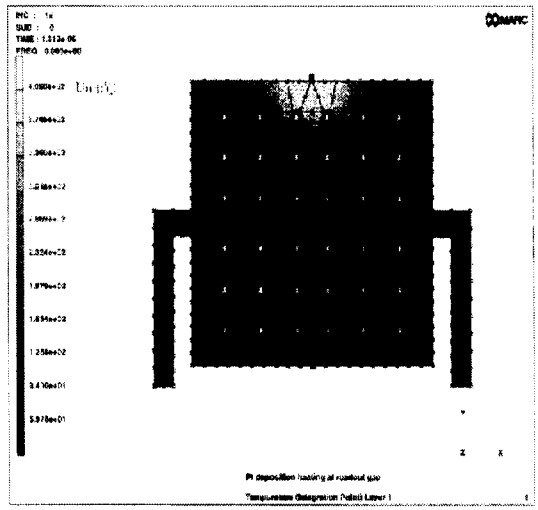

Fig. 7 Temperature distribution after 1.3×10^{-6} sec of heating process for tunnel gap by Pt deposition

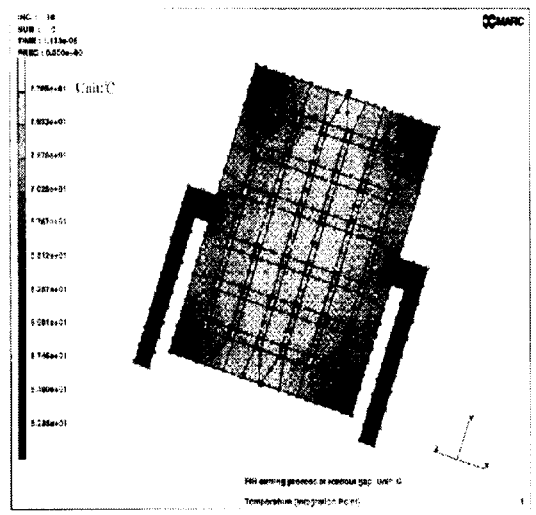

Fig. 8 Temperature distribution after $1.1. \times 10^{-4}$ sec cooling process for tunnel gap by FIB cutting

Fig. 8 shows a calculated temperature distribution of microaccelerometer during a FIB cut cooling process after 1.1×10^{-6}sec. Temperature gradients steep in the suspended beam edges and the corner of paddle.

Fig. 9 shows the temperature distributions of FIB cutting (90°) cooling process at additional beam for preventing a sticking problem. The center of paddle part becomes about 5~20℃ higher than the corner of paddle and suspended beam edges.

In Fig. 10, shows temperature contours representing the

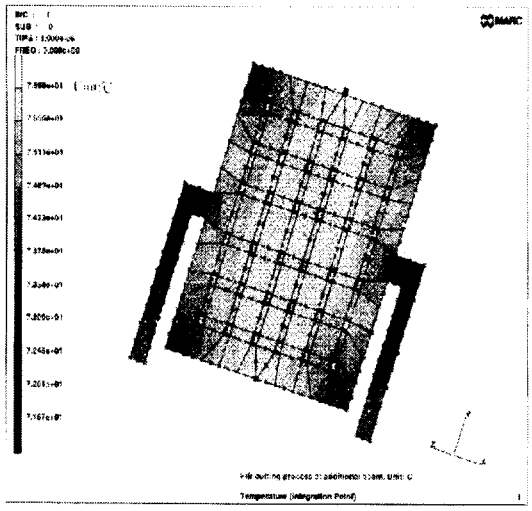

Fig. 9 Temperature distribution after 1.0×10^{-6} sec of cooling process for additional beam by FIB cutting(90°)

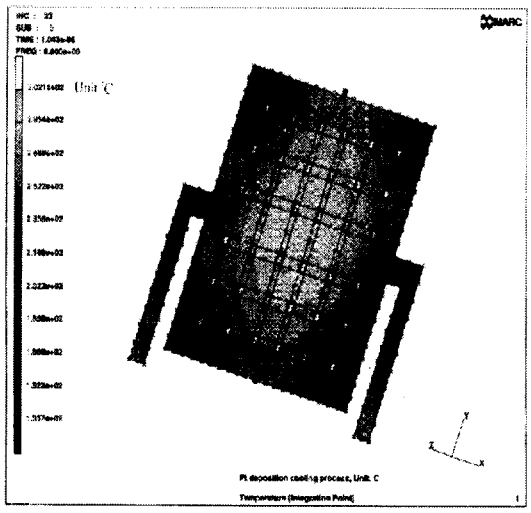

Fig. 10 Temperature distribution after 1.0×10^{-6}sec of cooling process for tunnel gap by Pt deposition

cooling process of Pt deposition. Corner parts of the paddle and the suspended beams are subjected to more thermal loss due to their corner shape. To obtain a more uniform temperature distribution, thermal radiation should be provided to these corner parts.

5. CONCLUSIONS

One of major problems associated with the manufacturing processes of the microaccelerometer based on the tunneling current concept is temperature gradient. In this paper, we analyzed temperature and thermal behaviors occurred in the microaccelerometer during the FIB cutting process and the Pt deposition process.

Temperature rise sufficiently low at the suspended beams. Instead, larger temperature gradient can be seen at the bottom of paddle part. The center of paddle part becomes about 5~20℃ higher than the corner of paddle and suspended beam edges. Corner parts of the paddle and the suspended beams are subjected to more thermal loss due to their corner shape.

REFERENCES

(1) J. Bryzek, "Impact of MEMS Technology on Society", Sensors and Actuators, A 56, pp. 1~9, 1996.

(2) D. F. Moore, S. C. Burgess, H. Chiang, H. Klaubert, N. Shibaike and T. Kiriyama, "Micromachining and Focused Ion Beam Etching of Si for Accelerometer", Symposium on Micromachining and Microfabrication, SPIE, Vol. 2639, pp. 253~258, 1995.

(3) F. Pourahmadi, P. Barth and K. Petersen, "Modeling of Thermal and Mechanical Stresses in Silicon Microstructures", Sensors and Actuators, A21-A23, pp. 850~858, 1990.

(4) J. Y. Richard, "Micro-machining using a Focused Ion Beam", Vacuum, Vol. 44, No.3/4, pp. 353~360, 1993.

(5) S. Johansson, F. Ericson and J. Schweitz, "Influence of Surface Coatings on Elasticity, Residual Stresses, and Fracture Properties of Silicon Microelements", J. Appl. Phys, Vol. 65, Jan. pp. 122~128, 1989.

(6) K. W. Lee and K. D. Wise, "SENSIM : A Simulation Program for Solid-State Pressure Sensors", IEEE. Transactions on Electron Devices, ED-29, pp. 34~41, 1982 .

(7) S. Crary, O Juma and Y. Zhang, "Software Tools for Designers of Sensors and Actuator CAE Systems" , IEEE. Solid-state sensors and Actuators (Transducers 91), San Francisco, CA, USA, pp. 498~503, 1991.
(8) Kurt E. Petersen, "Silicon as a Mechanical Materials", Proc. of IEEE, Vol. 70 No. 5, May, pp. 420~452, 1982.
(9) S. Johansson, J. Schweitz, L. Tenerz and J. Tiren, "Fracture Testing of Silicon Microelements in situ in a Scanning Electron Microscope", J. Appl. Phys., Vol. 63(10), May, pp. 4799~4805, 1988.
(10) F. Ericson and J. Schweitz, "Micromechanical Fracture Strength of Silicon", J. Appl. Phys., Vol. 68(11), 1 Dec. pp. 5840~5846, 1990.